SUPPLEMENTAL INFORMATION

The progression of replication forks at natural replication barriers in live bacteria

M. Charl Moolman[1‡], Sriram Tiruvadi Krishnan[1‡], Jacob W.J. Kerssemakers[1], Vincent Lorent[2], David J. Sherratt[3] and Nynke H. Dekker[1,⋆]

January 29, 2016

[1]Department of Bionanoscience, Kavli Institute of Nanoscience, Faculty of Applied Sciences, Delft University of Technology, Lorentzweg 1, 2628 CJ Delft, The Netherlands

[2]Université Paris 13, Sorbonne Paris Cité, Laboratoire de Physique des Lasers, CNRS, (UMR 7538), F-93430, Villetaneuse, France

[3]Department of Biochemistry, University of Oxford, Oxford OX1 3QU, United Kingdom

[‡]These authors contributed equally to this work.

[⋆]Corresponding author

Email address of the corresponding author: N.H.Dekker@tudelft.nl

1 Supplementary Experimental Procedures

1.1 Construction and characterization of fluorescent fusion strains

All strains are derived from the *E. coli* K 12 AB 1157 (1). The strains used for this study were constructed by λ-red recombination (2) or P1-transduction (3). A summary of the plasmids and strains used in this study are provided in Supplementary Tables 2 and 3.

1.1.1 Δ*Tus* in WT AB1157

Utilizing λ-red recombination we created a ΔTus mutant in WT AB1157 by knocking out the open reading frame of the *tus* gene. The plasmid pKD13 (GenBank: AY048744.1) was used as a template plasmid for amplifying the FRT flanked kanamycin resistance gene (*kanR*) sequence used during λ-red recombination. The primer sequences used were: Forward 5' – CCA CGA CTG TGC TAT AAA ATA AGT ATG TTG TAA CTA AAG TGG TTA ATA TTT GTA GGC TGG AGC TGC TTC G – 3'; Reverse 5' – GAC AGC TGG GTA CGG CCA GAA CAG ATG GTC GGC AGT ATG AAA GCC GGG CGA TTC CGG GGA TCC GTC GAC C – 3'. The DNA fragment was gel purified, and $\sim$ 700 ng of the linear DNA was used during electroporation of AB1157 cells over expressing the λ-red proteins from pKD46 (2). The correct insertion of the fragment into the chromosome of the resulting strain was assayed by PCR. The oligonucleotides used were 5' – GCG CAC GAT GGT CAA GTC AC – 3' and 5' – TAC GGC CAG AAC AGA TGG TC – 3'. The sequence of the deleted region in this strain was verified and confirmed by DNA sequencing.

1.1.2 *YPet-dnaN:tetR-mCerulean* (*oriC-dnaN*)

The *YPet-dnaN:tetR-mCerulean* (*oriC*) strain was constructed previously as described in *Moolman et al* (4).

1.1.3 *YPet-dnaN:tetR-mCerulean:*Δ*Tus* (*oriC-dnaN:*Δ*Tus*)

The *oriC:*Δ*Tus* was constructed using P1 transduction. Firstly, the FRT flanked *kanR* gene in the *oriC* strain, used during previous recombineering, was recombined out using the temperature the sensitive Flippase (FLP) enzyme expressed from the pCP20 plasmid as described elsewhere (2). Subsequently, the FRT flanked *kanR* gene from the Δ*Tus* strain was transduced into the *oriC* strain. The presence of the Δ*tus* knock-out was verified using the oligonucleotides: 5' – GCG CAC GAT GGT CAA GTC AC – 3' and 5' – TAC GGC CAG AAC AGA TGG TC – 3'. The sequence of the deleted region was confirmed by DNA sequencing.

1.1.4 *YPet-DnaN:oriZ* (*oriZ-dnaN*)

The *oriZ-dnaN* strain was constructed previously as described in (5).

1.1.5 *YPet-DnaN:oriZ:*Δ*Tus*(*oriZ-dnaN:*Δ*Tus*)

The *oriZ-dnaN:*Δ*Tus* was constructed using P1 transduction. Firstly, the FRT flanked *kanR* gene in the *oriZ* strain, used during previous recombineering, was recombined out using the temperature the sensitive Flippase (FLP) enzyme expressed from the pCP20 plasmid as described elsewhere (2). Subsequently, the FRT flanked *kanR* gene from the Δ*Tus* strain was transduced by P1 transduction into the out-recombined *oriZ-dnaN* strain. The presence of the Δ*tus* knock-out was verified using the oligonucleotides: 5'– GCG CAC GAT GGT CAA GTC AC – 3' and 5' – TAC GGC CAG AAC AGA TGG TC – 3'. The correct deletion of the *tus* gene at the desired region was confirmed by DNA sequencing.

1.1.6 *dnaQ-YPet:oriZ* (*oriZ-dnaQ*)

The *oriZ-dnaQ* was constructed using P1 transduction. The dnaQ-YPet gene from the previously constructed *dnaQ-YPet* strain (6) was transduced by P1 transduction into the

oriZ strain (5). For clarity this is the strain without any replisome component labelled. The presence of the *dnaQ-YPet* knock-out was verified using the oligonucleotides: 5' – AAT GAC CGC TAT GAG CAC TG – 3' and 5' – TTG CCT CGA CCT TCG TCA AC – 3'.

1.2 M9 growth medium used in experiments

1 L of M9 growth medium used in the experiments contains 10.5 g/L of autoclaved M9 broth (Sigma-Aldrich); 0.1 mM of autoclaved $CaCl_2$ (Sigma-Aldrich); 0.1 mM of autoclaved $MgSO_4$ (J.T.Baker); 0.3 % of filter-sterilized glycerol (Sigma-Aldrich) as carbon source; 0.1 g/L of filter-sterilized 5 amino acids, namely L-threonine, L-leucine, L-proline, L-histidine and L-arginine (all from Sigma-Aldrich) and 10 μL of 0.5 % filter-sterilized Thiamine (Sigma-Aldrich).

1.3 Microfluidic device fabrication

Cells are immobilized for imaging utilizing our version (7) of a previously reported microfluidic device (8). A detailed description of the fabrication procedure can be found in (7). In brief, electron-beam lithography in combination with dry etching techniques is used to fabricate the structures into a silicon wafer. This wafer is subsequently used to realize a negative mold of the structures with polydimethylsiloxane (PDMS). The resulting PDMS mold is then employed to successfully fabricate the positive structures with PDMS. Subsequently a cover glass is attached, and the device is used for time-lapse experiments.

1.4 Preparation of cells for microscopy

Cells were streaked onto Luria-Bertani (LB)-plates containing the appropriate antibiotics. Single colonies from these plates were grown in M9 supplemented with 0.3 % glycerol (Gly), essential nutrients (Supplementary Section 1.2), and with the appropriate antibi-

otics overnight at 37 °C with shaking. The following day, the cells were sub-cultured into the same medium and grown at 37 °C with shaking until an $OD_{600} \sim 0.2$ was reached. Cells were concentrated by centrifugation for 2 min at 16 100 g. The supernatant of the concentrated cells was decanted, and the pellet was resuspended in 50 μL M9-Gly with essential nutrients and injected into the microfluidic device. After injection into the device, the device was centrifuged for 10 min at 2500 g (Eppendorf 5810R). This centrifugation step assists the loading of the cells into the growth channels. Following centrifugation the device was mounted on the microscope with tubing attached to the inlet and outlet and incubated for $\sim$ 45 min at 37 °C. After incubation, fresh M9-Gly with essential nutrients (Supplementary Section 1.2) and the appropriate antibiotics are flushed through the device. The syringe containing the medium is subsequently attached to an automated syringe pump that continuous injects fresh M9-Gly, essential nutrients and 0.2 mg/mL bovine serum albumin (BSA) into the device at a rate of 0.5 mL/hr.

1.5 Microscope setup

Microscopy data were acquired on a commercial Nikon Ti microscope equipped with a custom-built laser excitation scheme similar to that reported previously (4). In brief, a Nikon CFI Apo TIRF 100x, 1.49 NA oil immersion objective is used for excitation and detection. A standard Nikon brightfield halogen lamp and condenser components are used for imaging cell outlines. Excitation is performed using a Cobolt Fandango 515 nm continuous wave (CW) diode-pumped solid-state (DPSS) laser for YPet, Cobolt Jive 561 nm CW DPSS laser for mCherry, and a Cobolt Twist 457 nm CW DPSS laser for mCerulean. The laser beams are combined using dichroic mirrors (Chroma 575dcspxr, zt457dcrb) and subsequently coupled into a single-mode optical fiber (KineFLEX). The output of the fiber is expanded and focused onto the back focal plane of the objective mounted on the microscope. Notch filters (Semrock NF03-514E, NF03-561E) were used to eliminate any laser

light leaking onto the camera. The emission of the different fluorescent proteins are projected onto the central part of an Andor iXon 897 Electron Multiplying Charge Coupled Device (EMCCD) camera using custom filter sets: Chroma z561, ET605/52m, zt561rdc (mCherry), Chroma z514, ET540/30m, zt514rd (YPet), Chroma z457/10x, ET490/40m, zt457rdc (mCerulean). A custom design commercial temperature control housing (Okolabs) is enclosing the microscope body is regulate the temperature at 37 °C. Sample position was controlled with a Nikon stage (TI-S-ER Motorized Stage Encoded, MEC56100) together with the Nikon Perfect Focus System (PFS) to eliminate Z-drift during image acquisition. A personal computer (PC) running Nikon NIS elements software is used for controlling the acquisition.

1.6 Time-lapse data acquisition

All data acquisition was performed on the previously described microscope in combination with a standard PC running Nikon NIS-elements (Supplementary Information Section 1.5). The order and type of fluorescence excitation was dependent on the strain being imaged.

For *oriC-dnaN* and *oriC-dnaN:*Δ*tus* cells, the cell outlines were imaged using standard brightfield illumination, and the YPet proteins were subsequently excited with the 515 nm laser line (80 ms exposure time). Time-lapse images were acquired every 2.5 min with the EMCCD gain set to 100.

For *oriZ-dnaN* and *oriZ-dnaN:*Δ*tus* cells, the cell outlines were again imaged using standard brightfield illumination, but different laser lines were used successively to excite the different fluorescent proteins. The sample was first excited with 515 nm (YPet), then 561 nm (mCherry) and lastly with 457 nm (mCerulean) with an exposure time of 80 ms in all the cases. The intensity for all the different measurement were kept constant. The inten-

sity of the 515 nm and 561 nm lasers was $\sim 5\,\mathrm{W}\cdot\mathrm{cm}^{-2}$, and the 457 nm laser was set to $\sim 2.5\,\mathrm{W}\cdot\mathrm{cm}^{-2}$. Intensity calibration was performed according to (9). Images were acquired every 2.5 min. Time-lapse acquisitions typically ran overnight, and spanning $\sim$ 10 hrs of measurement.

oriZ-dnaQ cells were imaged using the same procedure as for *oriZ-dnaN* cells expect that images were acquired every 5 min.

1.7 Data analysis

1.7.1 Localization of foci during replication

The acquired images were analyzed with custom-written MATLAB software (MathWorks) in combination with imageJ (10) as reported previously (4). Briefly, we correct for uneven background and illumination heterogeneity per image. Subsequently, we detect foci in each bacterium that have an intensity above the cytoplasmic fluorescence intensity as defined by the median of the total cytoplasmic signal. The detected foci are localized in each individual image by performing a maximum-likelihood estimation (MLE) of a two-foci Gaussian fit (11–13). The resulting fits are evaluated by rejecting the secondary fit if it is off-range, too weak compared to the brightest focus or to the total fluorescence intensity.

1.7.2 Time-resolved representation of foci positions

To study the temporal behavior of the replisome and chromosomal loci, it is crucial to be able to evaluate the process of focus separation during replication. Obtaining average values of focus separation is somewhat impeded by i) the wide spread for individual cells in the appearance of 'one focus' and 'two foci' observations and ii) the limited optical resolution to be able to discriminate one focus, from two closely adjacent ones. To minimize the influence of these factors, we proceed as follows when constructing averaged time-resolved position

traces as in Figure 3A, 4B of the main text. First, for each individual cell, we normalize the time axis such that $t = 0$ corresponds to the moment of initiation, as determined from the first emergence of a focus, and that $t = 1$ amounts to the last time point that one or two foci are observed. Secondly, we plot the average position for the cases of one or two foci respectively per normalized time. The size of the marker represents the percentage of cells found in this state.

1.8 Calculating the average replisome velocity during replication

We calculate the average replisome velocity in our experimental conditions by making use of the average replication time $t_{\mathrm{rep,oriC}} \sim 70\,\mathrm{min}$ (Supplementary Information Figure S4B) in combination with the size of the *E. coli* genome (4.6 Mbp). This results in a velocity of $v_{\mathrm{rep}} \sim 550\,\mathrm{bp/s}$ for an individual replisome under our experimental conditions.

Supplementary References

[1] Bachmann, B. J., 1972. Pedigrees of some mutant strains of Escherichia coli K-12. *Bacteriological Reviews* 36:525–557.

[2] Datsenko, K. A., and B. L. Wanner, 2000. One-step inactivation of chromosomal genes in Escherichia coli K-12 using PCR products. *Proceedings Of The National Academy Of Sciences Of The United States Of America* 97:6640–6645.

[3] Thomason, L. C., N. Costantino, and D. L. Court, 2007. E. coli genome manipulation by P1 transduction. *Current protocols in molecular biology* Chapter 1:Unit 1.17.

[4] Moolman, M. C., S. T. Krishnan, J. W. J. Kerssemakers, A. van den Berg, P. Tulinski, M. Depken, R. Reyes-Lamothe, D. J. Sherratt, and N. H. Dekker, 2014. Slow unloading leads to DNA-bound β2-sliding clamp accumulation in live Escherichia coli cells. *Nature communications* 5:5820.

[5] Wang, X., C. Lesterlin, R. Reyes-Lamothe, G. Ball, and D. J. Sherratt, 2011. Replication and segregation of an Escherichia coli chromosome with two replication origins. *Proceedings Of The National Academy Of Sciences Of The United States Of America* 108:E243–50.

[6] Reyes-Lamothe, R., D. J. Sherratt, and M. C. Leake, 2010. Stoichiometry and architecture of active DNA replication machinery in Escherichia coli. *Science* 328:498–501.

[7] Moolman, M. C., Z. Huang, S. T. Krishnan, J. W. J. Kerssemakers, and N. H. Dekker, 2013. Electron beam fabrication of a microfluidic device for studying submicron-scale bacteria. *Journal of nanobiotechnology* 11:12.

[8] Wang, P., L. Robert, J. Pelletier, W. L. Dang, F. Taddei, A. Wright, and S. Jun, 2010. Robust Growth of Escherichia coli. *Current biology* 20:1099–1103.

[9] Grünwald, D., S. M. Shenoy, S. Burke, and R. H. Singer, 2008. Calibrating excitation light fluxes for quantitative light microscopy in cell biology. *Nature protocols* 3:1809–1814.

[10] Schneider, C. A., W. S. Rasband, and K. W. Eliceiri, 2012. NIH Image to ImageJ: 25 years of image analysis. *Nature Methods* 9:671–675.

[11] Thompson, R. E., D. R. Larson, and W. W. Webb, 2002. Precise nanometer localization analysis for individual fluorescent probes. *Biophysical Journal* 82:2775–2783.

[12] Smith, C. S., N. Joseph, B. Rieger, and K. A. Lidke, 2010. Fast, single-molecule localization that achieves theoretically minimum uncertainty. *Nature Methods* 7:373–375.

[13] Mortensen, K. I., L. S. Churchman, J. A. Spudich, and H. Flyvbjerg, 2010. Optimized localization analysis for single-molecule tracking and super-resolution microscopy. *Nature Methods* 7:377–381.

[14] Reyes-Lamothe, R., C. Possoz, O. Danilova, and D. J. Sherratt, 2008. Independent Positioning and Action of Escherichia coli Replisomes in Live Cells. *Cell* 133:90–102.

SUPPLEMENTARY FIGURE LEGENDS

Figure S1. Representative temporal montages of the YPet-DnaN and *ori1*-mCherry signals for a complete replication cycle. (A-B) Montages for *oriZ-dnaN* cells. (A) YPet-DnaN montage and (B) *ori1*-mCherry montage. (C-D) Montages for *oriZ-dnaN:*Δ*Tus* cells. (C) YPet-DnaN montage and (D) *ori1*-mCherry montage. Scale bars, 3 μm.

Figure S2. Focus doubling time of the *R2*-mCerulean locus. (A) A representative *R2*-mCerulean fluorescent signal. (left) The kymograph of the *R2*-mCerulean locus for one complete replication cycle constructed by summation of the pixel intensities perpendicular to the long axis of the cell. (right) The *R2*-mCherry trace shown (left) determined from the Gaussian fitted positions from individual images for each time point. Images were acquired every 2.5 min during a time-lapse experiment. (B) The distribution of the time point during replication when the *R2*-mCerulean focus doubles. The mean doubling time of *R2*-mCerulean is $t_{\mathrm{doubling}} = 17 \pm 5$ min. (Error is $\pm$ SD, $\mathrm{n_{cells}} = 167$). (Inset) Schematical illustration indicating that the *R2*-mCerulean region has been replicated.

Figure S3. Replisome dynamics as measured in the *oriZ-dnaQ* strain. (A) The percentage of cells that have a single focus (light green line), double foci (dark green line) and no foci (black line) as function of replication time. It is evident that the percentage of cells having a single focus or double foci is roughly equally distributed throughout the replication process ($\mathrm{n_{cells}} = 43$). The transparent red rectangle indicates the time when *ori1*-mCherry focus doubles spatially. The width of the rectangle is $\pm$ SD. The SD is larger for *oriZ-dnaQ* compared to *oriZ-dnaN* due the frame rate being 5 min instead of every 2.5 min per image. (B) The intensity distributions of DNA-bound DnaQ-YPet prior (grey) and post (red) spatial doubling of the *ori1*-mCherry focus. $I_{\mathrm{prior},ori1-\mathrm{mCherry}} = 1.88 \cdot 10^4 \pm 2.25 \cdot 10^4$ counts

($n_{foci} = 278$), $I_{post,ori1-mCherry} = 1.79 \cdot 10^4 \pm 1.01 \cdot 10^4$ counts (mean ± SD, $n_{foci} = 608$). The difference between the means of the two distributions is $< 6\%$. While the error bars are more substantial for this DnaQ-YPet experiment compared to the YPet-DnaN epxeriment, a result of lower signal and reduced statistics. The mean number of DNA-bound DnaQ-YPet thus appears unchanged after *ori1*-mCherry has been replicated, i.e. after the CW replisome has encountered the Tus-*terC* roadblock.

Figure S4. Replication in *oriC-dnaN* and *oriC-dnaN:*Δ*Tus* characteristics. (A) Distribution of the division time for WT AB1157 cells. The average division time is $t_{div,AB1157} = 83 \pm 16\,\text{min}$ (Error is ± SD, $n_{cells} = 125$). (B) Distribution of the division time (brown) and replication time (purple) for *oriC-dnaN* cells. The average replication time $t_{rep,oriC-dnaN} = 70 \pm 7\,\text{min}$, and the average division time $t_{div,oriC-dnaN} = 85 \pm 15\,\text{min}$ (error is ± SD, $n_{cells} = 110$). (C) Distribution of the division time (brown) and replication time (purple) for *oriC-dnaN:*Δ*Tus* cells. The average replication time $t_{rep,oriC-dnaN:\Delta Tus} = 80 \pm 11\,\text{min}$, and the average division time $t_{div,oriC-dnaN:\Delta Tus} = 96 \pm 19\,\text{min}$ (error is ± SD). (D) Replisome dynamics for *oriC-dnaN* and *oriC-dnaN:*Δ*Tus* cells. Time-resolved traces of (left) *oriC-dnaN*, and (right) *oriC-dnaN:*Δ*Tus* cells. Here we plot a single DnaN-YPet focus (filled circles) and double DnaN-YPet foci (empty circles). The size of an individual circle at each time point is representative of the percentage of cells having that particular distribution of foci. The traces have been aligned with respect to initiation and termination of replication and binned. (E) The percentage of cells having a single focus (light green line), double foci (dark green line), and no foci (black line) as function of replication time. It is evident that the percentage of cells having a single focus or double foci is roughy equal for (left) *oriC-dnaN* and (right) *oriC-dnaN:*Δ*Tus* cells.

Figure S5. SCA patterns. (A-B) The fitted spatial intensity distributions in a minority of the cells. (A) *ori1*-mCherry and *R2*-mCerulean foci *spatially* overlapped. (B)

RLRL configuration, which is symmetric and taken to be equal to LRLR. The insets in (A) and (B) are schematic depictions of the different chromosomal loci patterns. (C) The observed SCA pattern determined at the time point when replication was half way.

SUPPLEMENTARY FIGURES

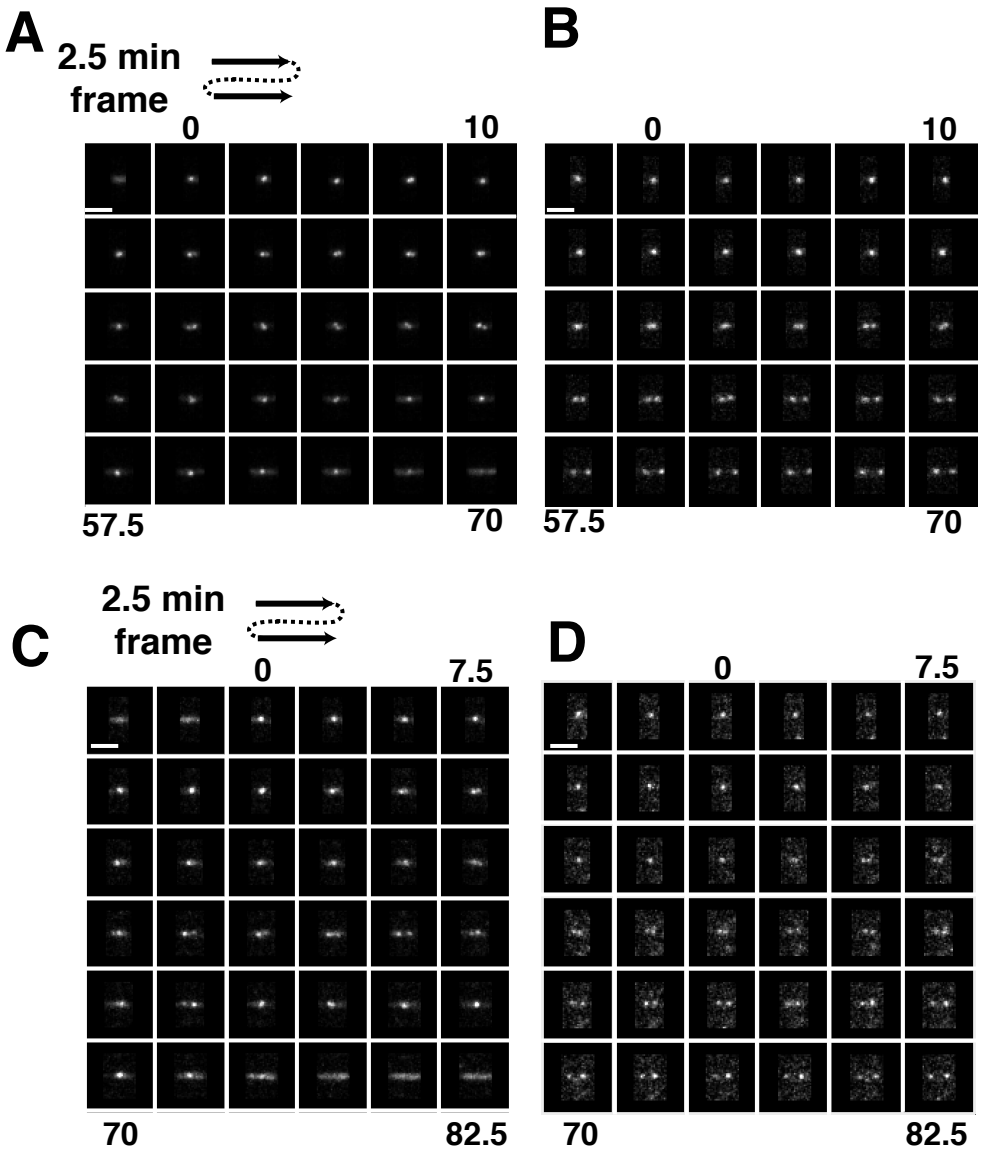

Figure S1

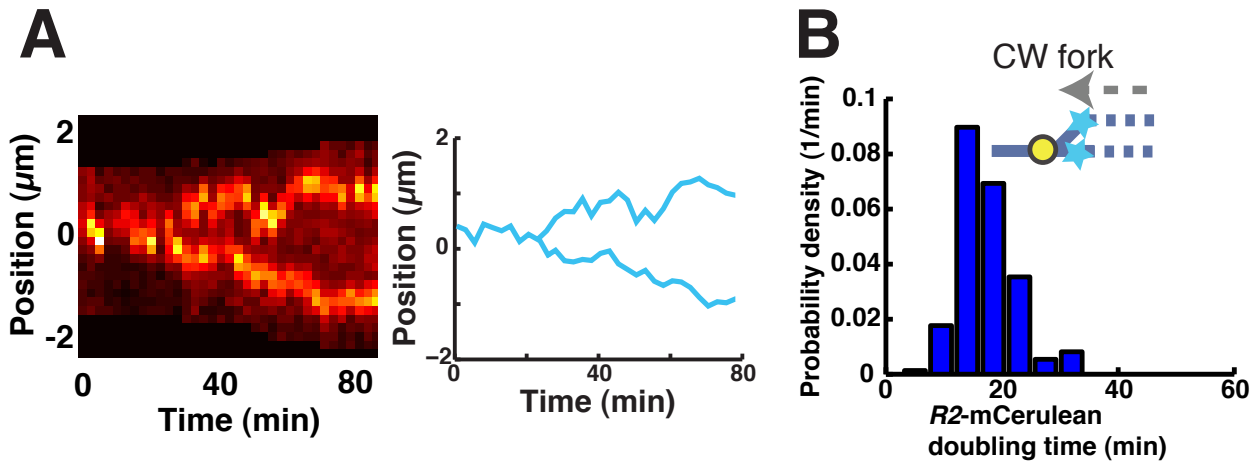
A
Position (μm)
2
0
-2
0
40
80
Time (min)
Position (μm)
2
0
−2
0
40
80
Time (min)
B
CW fork
Probability density (1/min)
0.1
0.08
0.06
0.04
0.02
0
0
20
40
60
R2-mCerulean
doubling time (min)

Figure S2

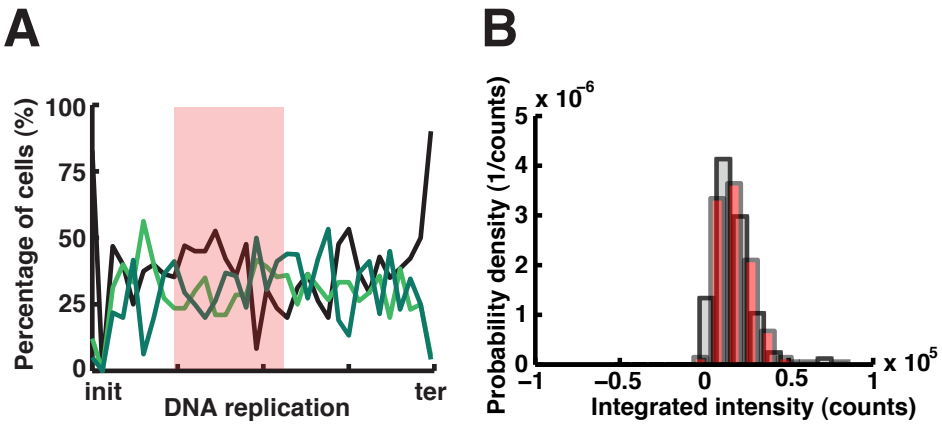
A
B
Percentage of cells (%)
100
75
50
25
0
init
DNA replication
ter
x 10^-6
5
4
3
2
1
0
Probability density (1/counts)
−1
−0.5
0
0.5
1
x 10^5
Integrated intensity (counts)

Figure S3

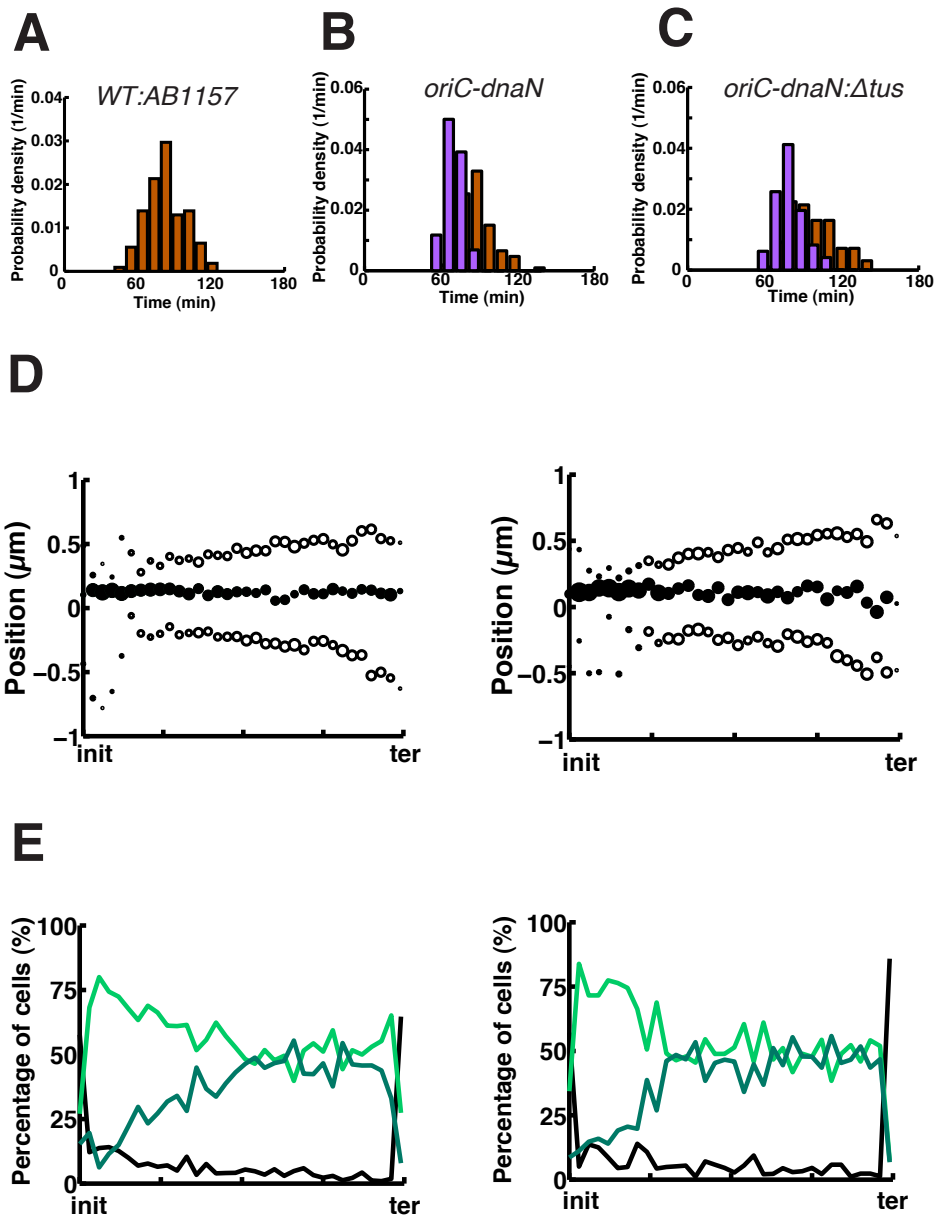
A
WT:AB1157
Probability density (1/min)
0.04
0.03
0.02
0.01
0
0
60
120
180
Time (min)
B
oriC-dnaN
Probability density (1/min)
0.06
0.04
0.02
0
0
60
120
180
Time (min)
C
oriC-dnaN:Δtus
Probability density (1/min)
0.06
0.04
0.02
0
0
60
120
180
Time (min)
D
Position (μm)
1
0.5
0
−0.5
−1
init
ter
Position (μm)
1
0.5
0
−0.5
−1
init
ter
E
Percentage of cells (%)
100
75
50
25
0
init
ter
Percentage of cells (%)
100
75
50
25
0
init
ter

Figure S4

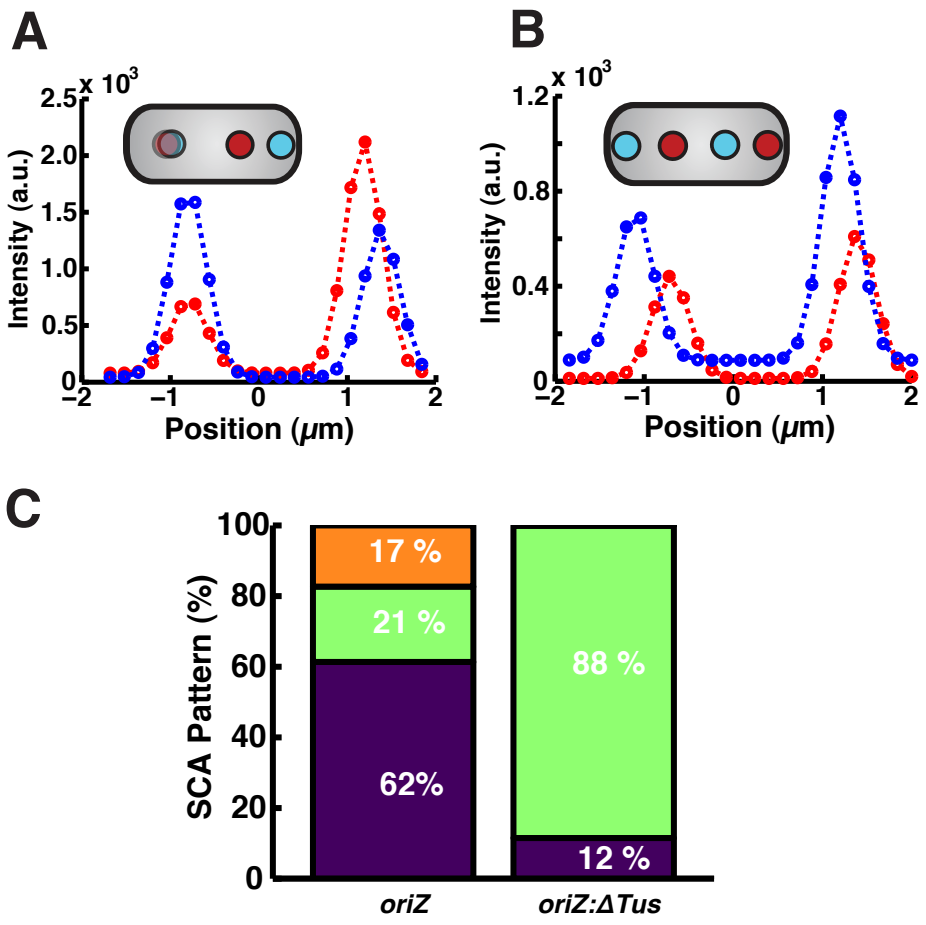
A
x 10^3
2.5
2.0
1.5
1.0
0.5
0
Intensity (a.u.)
−2
−1
0
1
2
Position (μm)
B
x 10^3
1.2
0.8
0.4
0
Intensity (a.u.)
−2
−1
0
1
2
Position (μm)
C
100
80
60
40
20
0
SCA Pattern (%)
17 %
21 %
62%
88 %
12 %
oriZ
oriZ:ΔTus

Figure S5

SUPPLEMENTARY TABLES

Frames prior and post *ori1* doubling	$I_{\text{prior},\textit{ori1}-\text{mCherry}}$	$I_{\text{post},\textit{ori1}-\text{mCherry}}$
2	$1.44 \cdot 10^5 \pm 6.16 \cdot 10^4$	$1.42 \cdot 10^5 \pm 6.52 \cdot 10^4$
5	$1.41 \cdot 10^5 \pm 6.18 \cdot 10^4$	$1.41 \cdot 10^5 \pm 6.80 \cdot 10^4$
10	$1.42 \cdot 10^5 \pm 6.53 \cdot 10^4$	$1.39 \cdot 10^5 \pm 6.83 \cdot 10^4$

Supplementary Table S1: Average intensities of DNA-bound YPet-DnaN prior and post spatial doubling of the *ori1*-mCherry focus. The numbers specified indicate the mean ± SD.

Plasmids	**Relevant genotype**	Construction
pKD46	Plasmid with λ-Red recombinase genes expressed under arabinose promoter	Created by standard cloning (2)
pCP20	Temperature sensitive plasmid with constitutively expressing flippase (FLP) enzyme.	Created by standard cloning (2)
pKD13	Template plasmid containing the FRT flanked kanamycin resistance gene (kanR) sequence.	Created by standard cloning (2)

Supplementary Table S2: Summary of different plasmids used in this study.

Strains	**Relevant genotype**	Construction
BN1110	AB1157 strain containing pKD46 plasmid	*E. coli* K-12 derivative (14)
BN1219	*YPet-dnaN* and *tetR-mCerulean*	P1-phage transduction (4)
BN1516	*kanR* gene recombined out	FLP/*FRT* recombination.
BN1598	Δ*Tus*	λ-red recombination: *FRT-kanR-FRT* from pKD13→BN1110
BN1868	*oriC-dnaN:*Δ*Tus*	P1-phage transduction: BN1598→BN1516
BN1861	*Ypet-DnaN*, Δ*oriC*, and Δ*oriZ*	P1-phage transduction (5)
BN1869	*oriZ-dnaN* with the *kanR* gene out recombined	FLP/*FRT* recombination
BN2111	*oriZ-dnaN:*Δ*Tus*	P1-phage transduction: BN1598 → BN1869
BN2381	*oriZ-dnaQ*	P1-phage transduction *dnaQ-YPet* → oriZ without a replisome marker (5)

Supplementary Table S3: Summary of different strains used in this study.